Environmental impacts of shifts in energy, emissions, and urban heat island during the COVID-19 lockdown across Pakistan

Ghaffar Ali [a], Sawaid Abbas [b, d, *], Faisal Mueen Qamer [c, **], Man Sing Wong [b, d], Ghulam Rasul [c], Syed Muhammad Irteza [e], Naeem Shahzad [b]

[a] College of Management, Shenzhen University, Nanhai Ave 3688, Shenzhen, 518060, China
[b] Department of Land Surveying and Geo-Informatics, The Hong Kong Polytechnic University, Hong Kong, China
[c] International Center for Integrated Mountain Development (ICIMOD), Kathmandu, 44700, Nepal
[d] Research Institute for Sustainable Urban Development, The Hong Kong Polytechnic University, Hong Kong, China
[e] Remote Sensing, GIS and Climatic Research Lab (RSGCRL), National Center of GIS and Space Applications, University of the Punjab, Lahore, Pakistan

ARTICLE INFO

ABSTRACT

Restrictions on human and industrial activities due to the coronavirus (COVID-19) pandemic have resulted in an unprecedented reduction in energy consumption and air pollution around the world. Quantifying these changes in environmental conditions due to government-enforced containment measures provides a unique opportunity to understand the patterns, origins and impacts of air pollutants. During the lockdown in Pakistan, a significant reduction in energy demands and a decline of ~1786 GWh (gigawatt hours) in electricity generation is reported. We used satellite observational data for nitrogen dioxide (NO_2), carbon monoxide (CO), sulphur dioxide (SO_2), aerosol optical depth (AOD) and land surface temperature (LST) to explore the associated environmental impacts of shifts in energy demands and emissions across Pakistan. During the strict lockdown period (March 23 to April 15, 2020), we observed a reduction in NO_2 emissions by 40% from coal-based power plants followed by 30% in major urban areas compared to the same period in 2019. Also, around 25% decrease in AOD (at 550 nm) thickness in industrial and energy sectors was observed although no major decrease was evident in urban areas. Most of the industrial regions resumed emissions during the 3rd quarter of April 2020 while the urban regions maintained reduced emissions for a longer period. Nonetheless, a gradual increase has been observed since April 16 due to relaxations in lockdown implementations. Restrictions on transportation in the cities resulted in an evident drop in the surface urban heat island (SUHI) effect, particularly in megacities. The changes reported as well as the analytical framework provides a baseline benchmark to assess the sectoral pollution contributions to air quality, especially in the scarcity of ground-based monitoring systems across the country.

© 2021 The Author(s). Published by Elsevier Ltd. This is an open access article under the CC BY-NC-ND license (http://creativecommons.org/licenses/by-nc-nd/4.0/).

1. Introduction

The global spread of COVID-19 is not only threatening public health (WHO, 2020) but the consequent lockdowns across the world as a preventative measure are damaging global economic growth (Maliszewska et al., 2020). The Asian Development Bank (ADB) has forecasted a global impact of USD156 billion or 0.2% of global gross domestic product (GDP) and noted that, in South Asia, it is expected to decrease sharply by 2.2% in 2020 (Asian Development Bank, 2020). Undoubtedly, the pandemic-led lockdown has caused global losses in both human and financial terms in addition to prolonged hardships while numerous challenges lie ahead. Nevertheless, the crisis also reminds us of the need to build a safer and more resilient world which can respond to any future biological crisis. The International Monetary Fund (IMF) has emphasized the promotion of green recovery through investments in cleaner transport, green technologies, sustainable agriculture, and climate resilience.

The current COVID-19 pandemic is to date the most devastating health crisis of our time and the greatest challenge that humanity

*Corresponding author. Department of Land Surveying and Geo-Informatics, The Hong Kong Polytechnic University, Hong Kong, China.
** Corresponding author.
E-mail addresses: sawaid.abbas@gmail.com, sabbas@polyu.edu.hk (S. Abbas), faisal.qamer@icimod.org (F.M. Qamer).

has had to face in the post-World War II era. Since its emergence in January 2020, the COVID-19 virus has spread to all the continents of the world except Antarctica. On March 11, 2020, the World Health Organization (WHO) formally announced the COVID-19 outbreak as a pandemic. With that declaration, as a measure to retard its spread, almost two billion people around the world were placed under a partial or complete lockdown significantly reducing the volume of transportation and bringing to a near-complete halt to industrial activities. In Pakistan, the first lockdown was declared in the province of Sindh on March 23, 2020, which was followed later by the other provinces and cities of the country.

On the environmental front, the implementation of lockdowns across the world has resulted in remarkable improvements in air quality (Yunus et al., 2020), wildlife sightings and water quality in additions to reductions in noise pollution (Kim et al., 2020). Negative outcomes in the form of environmental pollution are however not absent under pandemic conditions: for example, non-biodegradable waste generated by the increase in the use of surgical masks, gloves, and protective equipment as well as hospital residuals (Saadat et al., 2020). Researchers, who are trying to understand the factors that cause deadly air pollution around the world, have already established a link between mobility and air pollution (IQAir, 2019).

Air pollution is one of the most pronounced environmental risks to human health as well as to global economies (Sánchez-Triana et al., 2014). Pakistan is one of the rapidly urbanizing countries in South Asia showing/recording a steep growth in the transportation and industrial energy sectors. Historically, emissions from the industrial and transportation sectors have been a major contributor to air pollution in Pakistan (Shahid et al., 2015), a new contributor to which is fossil-fuel-based thermal energy plants (Alkon et al., 2019). As in other South Asian urban centres (Fatmi et al., 2020), air pollution is causing serious damage to public health and environmental quality in the metropolitan cities of Pakistan (Pilarczyk et al., 2019). According to Colbeck et al. (2010), Nitrogen dioxide (NO_2) and the particulate matter (PM) concentrations were higher than the optimal levels devised by the WHO. The WHO has noted that approximately 200 mortalities per 100,000 population are linked to environmental factors in Pakistan (Sánchez-Triana et al., 2014). Likewise, a 78% increase in anthropogenic SO_2 levels is reported during the period from 2005 to 2016 across Pakistan (Jabeen and Khokhar, 2019).

Monitoring aerosol optical depth (AOD) through satellite remote sensing provides an alternative means of measuring the PM concentrations at the ground level by modelling the relationships between AOD and PM (Bilal et al., 2017). However, an experimental study by Levy et al. (2010) suggested that a small percentage change in estimating AOD may lead to large differences in long term trends. Since 2010, global assessments of PM concentrations have been mostly made through a combination of satellite remote observations, chemical transport models, and ground measurements (Mao et al., 2014). For instance, Krishna et al. (2019) estimated $PM_{2.5}$ concentration over the Indian region from the space-based AOD observations. In Pakistan, several studies have demonstrated that Moderate Resolution Imaging Spectroradiometer (MODIS) based AOD measurements are useful in understanding the seasonal and spatial variations in aerosol concentrations with a reasonable degree of accuracy (Butt et al., 2018).

In 2017, with the launch of Copernicus Sentinel 5P, which has an advanced multispectral imaging spectrometer TROPOspheric Monitoring Instrument (TROPOMI), a new era in atmospheric gas measurements commenced making it possible to accurately measure a wide range of pollutants at higher spatial resolutions across the globe, such as in Finland (Ialongo et al., 2020), Turkey (Kaplan et al., 2019) and comparative assessment among different cities of

the world (Lama et al., 2019). TROPOMI is designed to monitor several atmospheric elements including NO_2, ozone (O_3), sulphur dioxide (SO_2), methane (CH_4), and carbon monoxide (CO) as well as surface ultraviolet (UV) radiation (Veefkind et al., 2012). It obtains information on atmospheric NO_2 concentrations by measuring the solar light backscattered by the atmosphere and the Earth's surface. Several studies have already combined ground-based instruments and satellite data to measure SO_2 (Shikwambana et al., 2020) and NO_2 (Omrani et al., 2020). Griffin et al. (2019) found that the TROPOMI's NO_2 vertical column densities are highly correlated with ground measurements with a negative bias of 15−30% in the Canadian oil sands areas. Another study has observed a 10% mean relative and absolute bias between the TROPOMI and ground-based NO_2 total columns (Ialongo et al., 2020).

The urban heat island (UHI) effect is a well-known phenomenon caused by the warmer temperature of developed urban areas concerning its surrounding or nearby rural environments with less infrastructural development. The difference in temperature arises due to proportion, proximity and potential of impervious and pervious surfaces in urban and rural environments to hold and absorb heat (Martin-Vide et al., 2015). Research indicates that, in recent years, its impacts on human health have been more pronounced during extreme summer weather conditions and major heatwave events (Nori-Sarma et al., 2019). A study by Zhu et al. (2017) has concluded that vehicular flows make a significant contribution to the UHI phenomenon. According to Chapman and Thornes (2005), heat is transmitted to the road surface by sensible heat and moisture fluxes from engine exhaust as well as frictional heat dissipation from tires. Given the lack of a mass transit system in the major cities of Pakistan, the number of vehicles on the road has recorded a steep annual growth rate of over 8.5% (Hussain et al., 2018). Apart from vehicular emissions and combustions, the emissions and heat generated in the industrial and power plant region also significantly influence the surface energy balances in cities (Phelan et al., 2015). Thus, understanding the impact of the territory-wide lockdowns on UHI can provide important insights on the relative contribution of different pollution-emitting sectors on the UHI phenomenon.

This study presents the remote sensing-based assessment of changes in NO_2, CO, SO_2, AOD and UHI effect associated with the lockdown implementations to retard the spread of the COVID-19 virus in Pakistan. The results presented here are timely and will not only contribute towards understanding the environmental dynamics and sectoral contributions of energy emissions but also towards measures to control their adverse impacts in Pakistan and other Asian countries with similar dynamics. Since the UHI analysis is based on Land Surface Temperature (LST) derived from satellite images therefore the UHI in this study refers to the Surface UHI (SUHI).

2. Materials and methods

2.1. Description of study area and selection of sites

We selected twenty locations across Pakistan for this study which were identified based on the spatial intersection of urban area clusters, NO_2 emission hotspots (derived from average conditions during 2019), and well-known industrial, gas field, power and cement plant sectors in Pakistan (Fig. 1). The study sites belong to five broad categories of emission sources: megacities (Karachi, Lahore, Faisalabad and Rawalpindi-Islamabad), major cities (Multan, Peshawar, Hyderabad and Quetta), industrial areas (Taxila and Sadiqabad), gas fields (Sui, Daharki and Ghotki), power plants
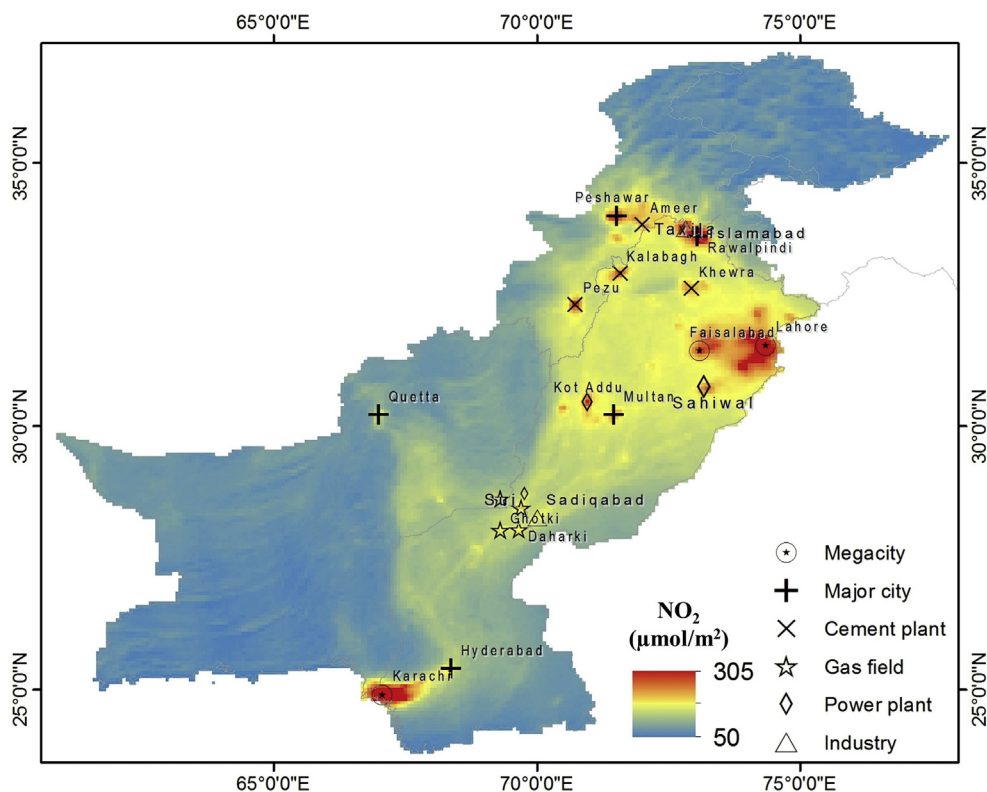
Fig. 1. Locations of selected sites overlaid on average tropospheric NO$_2$ concentration map.

(Kashmore, Kot Addu and Sahiwal), and cement plants (Pezu, Kalabagh, Khewra and Ameer).

2.2. Data used and pre-processing

The NO$_2$, SO$_2$, CO, AOD, and LST data used in the study were acquired during Jan 01 to May 15 for the years 2019 and 2020. The datasets were obtained and processed using the Google Earth Engine (GEE) API (Gorelick et al., 2017). The land use land cover compositions of the study sites (Fig. 2) are derived from the Copernicus Global Land Service: Land Cover 100 m (Buchhorn et al., 2019).

We used TROPOMI data to measure the changes in NO$_2$, SO$_2$, and CO (Veefkind et al., 2012). To ensure data quality, the data comes with a quality assurance band (qa_value) indicating quality of a pixel ranging from 0 (poor) to 1 (good) which is derived from numerous factors including presence of clouds, surface albedo, snow/ice pixels, signal saturation and geometry of acquisition. The Level 3 product in the GEE is produced at 0.01° spatial resolution from the Level 2 Sentinel 5P data (TROPMI, 2020) before ingesting in the GEE. The data is extensively filtered to remove poor quality pixels with 'qa_value' less than 0.75 for the 'tropospheric_NO2_column_number_density band of NO$_2$' while the other datasets (except for the O$_3$ and SO$_2$) are filtered by 'qa_value' less than 0.5 (S5P-GEE, 2020). The Level 3 data in the GEE is produced with a 'cloud_fraction' layer indicating probability of cloud presence in a given pixel which ranges from 0 (no clouds) to 1 (covered with clouds). To avoid misleading results, we removed the pixel with cloud cover probability of more than 0.2 for all the measurements. The native measurement unit of the tropospheric vertical column of NO$_2$, SO$_2$, and CO is mol/m^2 However, for the current assessment, the unit were converted to μmol/m^2.

The AOD at 550 nm is derived from the MODIS product MCD19A2-V6 (Lyapustin and Wang, 2018), a Level 2 product produced by Terra and Aqua combined Multi-angle Implementation of Atmospheric Correction (MAIAC) AOD that provides a wide range of spatial information with near-daily global coverage at 1 km spatial resolution (Levy et al., 2010). We used the quality tags layer, "AOD_QA", to retain good quality pixel ('Best quality' pixels using the "QA for AOD" mask) and clear pixels (removing pixels labelled as 'Possibly cloudy', 'Cloudy' and 'Cloud Shadow' using the "Cloud" mask).

To assess the SUHI conditions, we used the Terra MODIS daily night-time LST composites (MOD11A2) produced at 1 km resolution. The data is preprocessed to obtain the clear-sky pixels. Only pixels with an average LST error of less than or equal to 2 K are selected for further analysis. For this, the QA flags with integer values of 0, 1, 5, 64, 17, 21, 65, 69, 81, and 85 were retained while pixels having other quality tags were screened out (Neteler, 2010).

Existing datasets of dense human habitation (Corbane et al., 2017) derived from Sentinel 1 and Landsat satellite data at 30 m resolution were used for core urban area delineation. Spatially averaged SUHI effect was calculated for each of the sites (the bounding rectangle of each site) by taking the difference between the spatially averaged LST of the urban and surrounding non-urban pixels (excluding water pixels). The urban and non-urban area masks were developed from the Copernicus Global Land Service: Land Cover 100 m (Buchhorn et al., 2019) (Fig. 2).

2.3. Data analysis

A rigorous data analysis was performed to quantify changes in NO$_2$, CO, SO$_2$, AOD and SUHI induced by the lockdown. In our assessment, we took data on air pollution and SUHI conditions in the selected sites for the preceding year (2019) as a proxy for conditions during the "normal" and compared them with data for
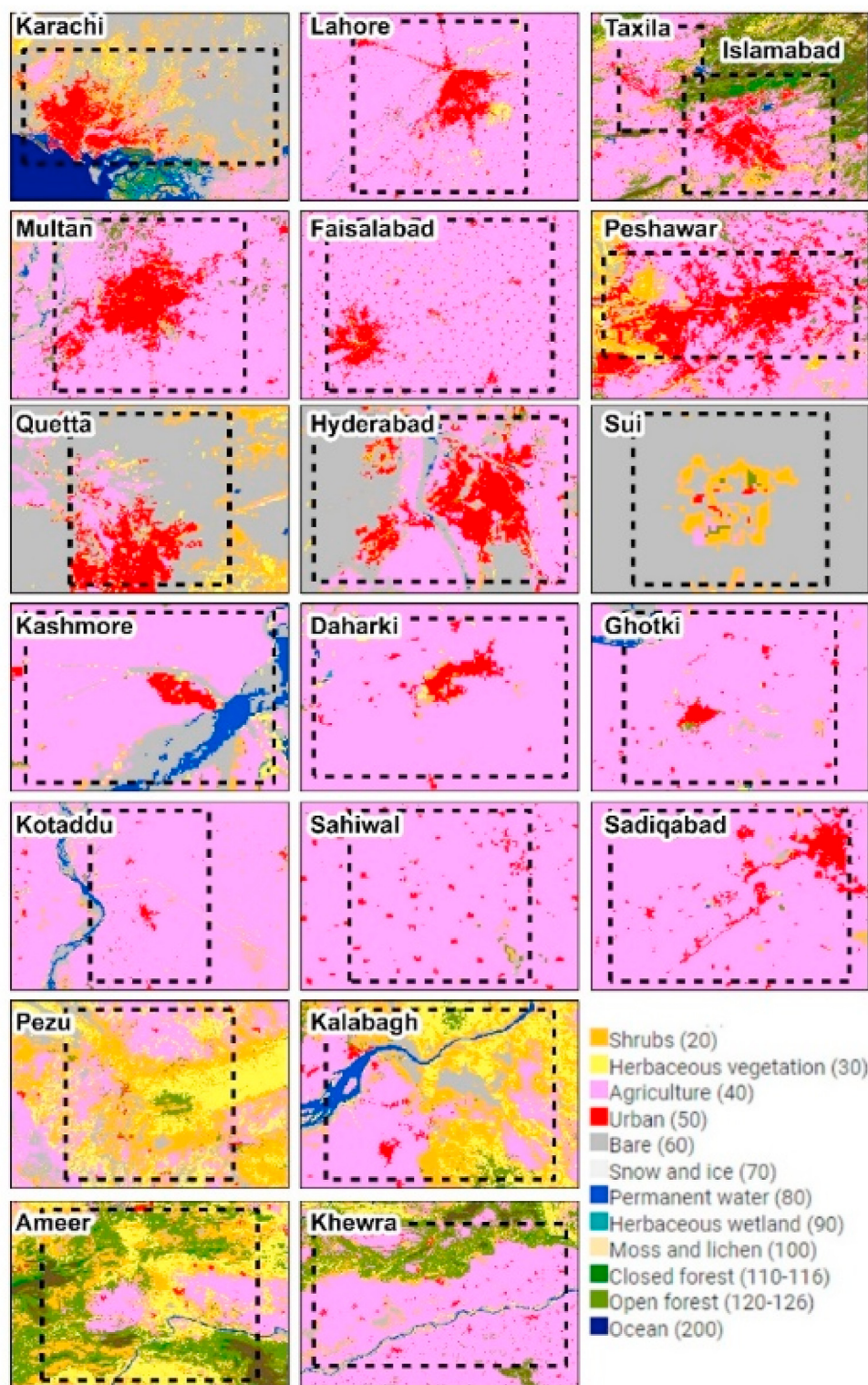
Fig. 2. Land cover land use composition of the study sites, the class names and codes retained according to the Copernicus Global Land Service: Land Cover 100 m.

the period under lockdown conditions. Also, a chronosequence analysis for the year 2020 was performed to identify the changes in the environmental factors in pre and during the lockdown. In Pakistan, the lockdown was first implemented on March 23, 2020 in the province of Sindh followed by a country-wide lockdown from March 25, 2020. But the policy relating to the lockdown has varied

vis-à-vis the residential and industrial sectors during different stages of the lockdown implementation. Therefore, we have divided the analytical framework into five distinct periods: P1 — Earlier (Jan and Feb); P2 — Pre-Lockdown (March 01 to March 22); P3 — During Lockdown (March 23 to April 15); P4 — Partial Loosening (April 16 to April 30); and P5 — Limited Lockdown (May 01 to

May 15). The P4 refers to partial loosening of the lockdown in when the industrial sectors started to operate. Later on, other commercial and business activities were resumed with a restriction under the limited lockdown. The non-parametric Wilcoxon Test was applied to determine the significant changes among the periods. A time series analysis was also performed to analyze temporal patterns from March 01 to May 15 for 2019 and 2020. These trends were fitted using a Local Polynomial Regression Fitting (loess) algorithm to elicit the overall temporal patterns. The temporal analysis was performed on spatially averaged values of the pollutants. The spatial aggregation was done by drawing rectangles around the selected location based on the NO_2 hotspots derived from the annual mean composite images of 2019.

Furthermore, maps were produced to portray spatial distribution at the country level and the selected sites. Air pollution conditions were assessed for all 20 sites by measuring NO_2, CO, SO_2, and AOD. Due to the relatively lesser amount of impervious surfaces in small cities (Fig. 2), the SUHI effect analysis was confined to mega-urban centres cities (Karachi, Lahore, Faisalabad, Multan, Peshawar, Hyderabad, Quetta and Islamabad) with greater than 1 million in population. The description, location, extent and land cover land use composition of the sites are given in Figs. 1 and 2. The data were processed on Google Earth Engine and the analysis was performed in R (R Core Team, 2020).

3. Results and discussion

To better understand the impacts of the lockdown on environmental conditions, we grouped the data into five periods: P1 — Earlier (Jan and Feb); P2 — Pre-Lockdown (March 01 to March 22); P3 — During Lockdown (March 23 to April 15); P4 — Partial Loosening (April 16 to April 30); and P5 — Limited Lockdown (May 01 to May 15). Table 1 presents a summary of the averaged/change statistics for NO_2, CO, SO_2, AOD and SUHI segregated by the key sectors - megacities, major cities, industrial areas, gas fields, power plants and cement plants.

3.1. Energy mix situation of Pakistan

Energy demand and supply is the backbone of all the economic sectors as the energy consumption is correlated with GDP growth of a country. The COVID-19 pandemic exacerbated the challenges of power generation, transmission and distribution system of Pakistan. The total installed power generation of Pakistan was 38,719 MW by June 2020 (NEPRA, 2020). The total energy generation capacity of the installed thermal power plants is 63%, followed by hydel (27.5%), renewable (5.8%) and nuclear (3.7%). During 2020, energy demand in the country was reduced due to the COVID-19 pandemic and nation-wide lockdown. This resulted in a decline of 1786.30 GWh electricity generation during 2019—2020, as compared to 136,532 GWh electricity generated during 2018—2019 (NEPRA, 2020). In 2020, Pakistan produced 56% of its energy generation requirements from thermal sources (oil, natural gas and coal power plants), 32% from hydel power plants, the remaining 12% is generated from nuclear (8%) and renewable energy (4%) (NEPRA, 2020). This use of different sources to generate electricity is referred to as "energy mix". Since strict lockdown was implemented in Pakistan from March 23 to April 25, 2020, 95% transportation and industrial sectors were shut down immediately. The lockdown was softened from May 2020 and emissions started to spike again "after lockdown situation". Forthcoming analyses are performed and presented to elaborate on the environmental changes due to shifts in energy consumption before and during the lockdown in Pakistan. It is assumed that major sources of greenhouse gas (GHGs) emissions were from energy consumption in industrial sectors including power plants, cement plants and other production units as well as all types of transportation.

3.2. Lockdown impact on NO_2

The time sequence maps for 2019 (Jan—May) indicate that the tropospheric column of NO_2 concentrations spread across Pakistan from north to south originating from urban and industrial sources in Rawalpindi-Islamabad, Lahore, and Peshawar in the north to Karachi in the south (Fig. 3). According to Zheng et al. (2019), the NO_2 concentration decreases with increasing temperature. However, the temporal patterns of NO_2 concentration over Pakistan show a relatively stable concentration from Jan to May (see Figs. 3 and 4). Nevertheless, a decrease in temperature and NO_2 was observed during the lockdown period in 2020. Megacities, including Karachi (84.4 $\mu mol/m^2$), Lahore (70.3 $\mu mol/m^2$), Islamabad-Rawalpindi (62.2 $\mu mol/m^2$) and Faisalabad (50.1 $\mu mol/m^2$) have the highest concentration of NO_2 (average: 66.7 $\mu mol/m^2$) followed by the coal-based thermal power plants (average: 60.1 $\mu mol/m^2$) in Kashmore (65.7 $\mu mol/m^2$), Sahiwal (62.2 $\mu mol/m^2$) and Kot Addu (52.4 $\mu mol/m^2$) (Table 1, Fig. 4). Notably, NO_2 emissions from single power plants in Sahiwal and Kot Addu are comparable to the total emissions over the megacities of Islamabad-Rawalpindi and Faisalabad (Table 1, Fig. 4).

Overall, a significant decrease in NO_2 emissions was observed during the lockdown periods in 2020 compared to the same periods in 2019 in all sectors. The highest decrease was observed over the power plant regions (40% decrease) followed by the megacities (37% decrease), major cities (23.5% decrease), industry (19% decrease) and gas fields (8% decrease) (Table 1).

Generally, satellite-based NO_2 concentrations portray a good correlation ($r = 0.68$) with the ground-based measurements. However, according to Ialongo et al. (2020), the TROPOMI total columns could underestimate NO_2 compared to ground-based observations. A review of the literature on NO_2 emissions in Pakistan suggests that the 48-h ground-based observations of NO_2 were highest in Peshawar followed by Islamabad, Lahore and Karachi in 2014 (Sánchez-Triana et al., 2014). However, according to findings in our study, Peshawar (41.7 $\mu mol/m^2$) ranks 7th among the eight mega and major cities of Pakistan (Table 1) concerning NO_2 emissions.

As the data reported above shows, the NO_2 emissions for 2020 were similar to those for 2019 during the periods of P1 - Earlier (Jan and Feb) and P2 — Pre Lockdown (March 01 to March 22). However, they show a substantial reduction during P3 — During Lockdown (March 23 to April 15) period. This decline in NO_2 emission is similar to that reported in other parts of the globe (Isaifan, 2020; Le Quéré et al., 2020; Zhang et al., 2020). In Pakistan, both urban transportation and industries remained halted for three weeks (P3 — During Lockdown from March 22 to April 15) until partial loosening of the lockdown in P4 (April 16 to April 30). Notably, much of the industrial emissions have picked up since April 16 (Fig. 4) reaching a similar level of emissions as reported before the lockdown in 2020 and the reference year of 2019 (Fig. 5-b). This is contrary to the emission patterns in mega and big cities where the lockdown has significantly reduced mobility in the cities as a result of which NO_2 emissions do not show full recovery by the P5 period (see Fig. 5-a). The analysis makes this evident where, despite transportation restrictions during the P4—P5 periods, a large amount of NO_2 emissions has already become visible in industrial cities like Karachi, Lahore and Faisalabad in comparison with non-industrial cities like Peshawar, Hyderabad and Quetta. With regard to location-specific observations, the gas field plant at Sui appears as the most stable point with no changes in emission of air pollutants between 2019 and 2020, the reason being that the Sui gas field which produces 604 million cubic feet daily of natural gas maintained its operations

Table 1

Summary of the changes observed in NO$_2$, AOD and SUHI in 2019 and 2020. The values temporally averaged from March 22 to April 30 covering the period of lockdown (P3) and partially relaxed lockdown (P4) in Pakistan.

| City/Sector	NO$_2$ (μmol/m^2)			AOD (550 nm)			SUHI (°C)		
	2020	2019	Change (%)	2020	2019	Change (%)	2020	2019	Change (%)
Megacities									
Karachi	56.7	84.4	−32.9	0.34	0.34	0.44	0.9	1.2	−21.7
Lahore	40.1	70.3	−42.9	0.32	0.34	−5.48	2.9	3.3	−9.3
Faisalabad	36.2	50.1	−27.8	0.29	0.35	−15.27	2.6	3.7	−29.2
Rawalpindi & Islamabad	34.7	*62.2*	*−44.1*	0.25	0.26	−2.37	*1.4*	*1.7*	*−17.9*
(average)	**41.9**	**66.7**	**−36.9**	**0.30**	**0.32**	**−5.67**	**2**	**2.4**	**−19.5**
Major cities									
Multan	41.6	45.2	−8.1	0.48	0.36	32.97	1.9	2.6	−18.6
Peshawar	32.8	41.7	−21.2	0.26	0.23	13.93	0.7	0.9	−10.5
Hyderabad	35.1	46.6	−24.7	0.42	0.35	18.62	1.1	1	5.4
Quetta	14.6	24.6	−40.6	0.21	0.22	−4.17	1	1.2	15
(average)	**31**	**39.5**	**−23.6**	**0.34**	**0.29**	**15.34**	**1.3**	**1.4**	**−8.7**
Industrial areas									
Taxila	37.7	54.8	−31.2	0.24	0.28	−13.13			
Sadiqabad	*42.9*	*46.3*	*−7.4*	0.27	0.43	−37.07			
(average)	**40.3**	**50.6**	**−19.3**	**0.26**	**0.35**	**−25.10**			
Gas fields									
Sui	36.8	38.4	−4.2	0.57	0.51	−44.86			
Daharki	41.2	44.7	−8	0.24	0.42	−42.73			
Ghotki	42.2	48.1	−12.3	0.52	0.52	0.62			
(average)	**40**	**43.7**	**−8.2**	**0.44**	**0.48**	**−28.99**			
Power plants									
Kashmore	38.3	65.7	−41.7	0.45	0.41	−45.19			
Kot Addu	30.2	52.4	−42.4	0.37	0.37	0.69			
Sahiwal	39.8	62.2	−36	0.26	0.34	−24.17			
(average)	**36.1**	**60.1**	**−40.1**	**0.36**	**0.37**	**−22.89**			
Cement plants									
Pezu	48.6	42.1	15.6	0.41	0.41	0.71			
Kalabagh	51.5	39.4	30.7	0.32	0.39	−17.96			
Khewra	28.7	34.3	−16.3	0.35	0.36	−2.31			
Ameer	29.1	35.1	5.1	0.28	0.30	−6.91			
(average)	**39.5**	**37.7**	**8.8**	**0.34**	**0.37**	**−6.62**			
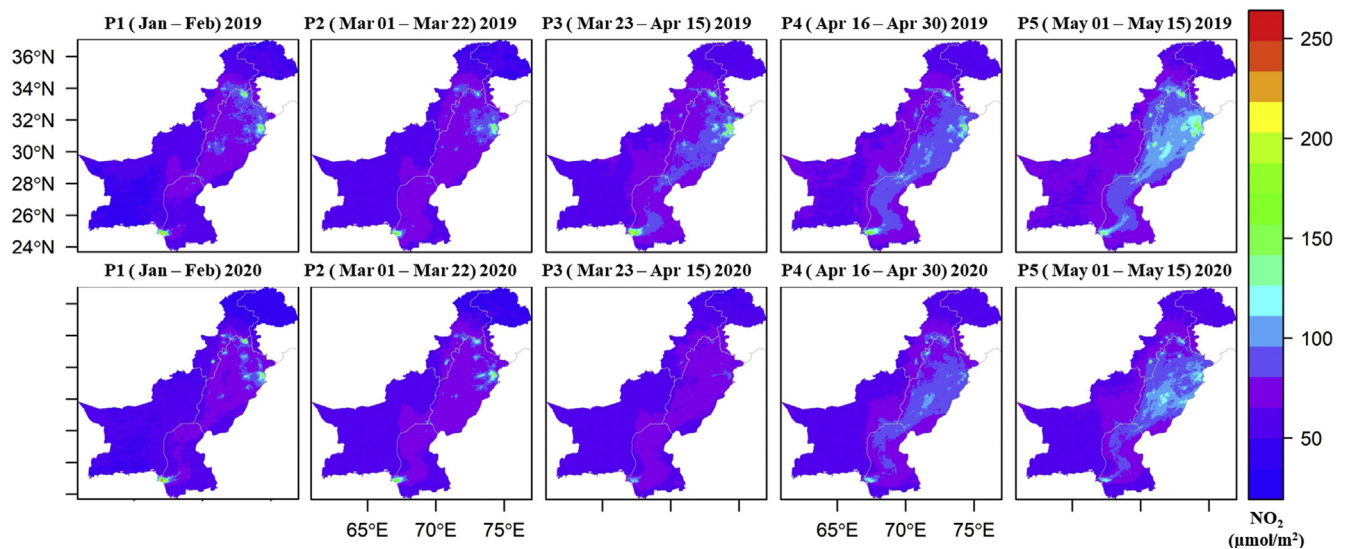
Fig. 3. The tropospheric NO$_2$ distribution over Pakistan during the five periods in 2019 and 2020. P1 - Earlier (Jan and Feb); P2 — Pre Lockdown (March 01 to March 22); P3 — During Lockdown (March 22 to April 16); P4 — Partial Loosening (April 16 to April 30); and P5 - Post-Lockdown (May 01 to May 15).
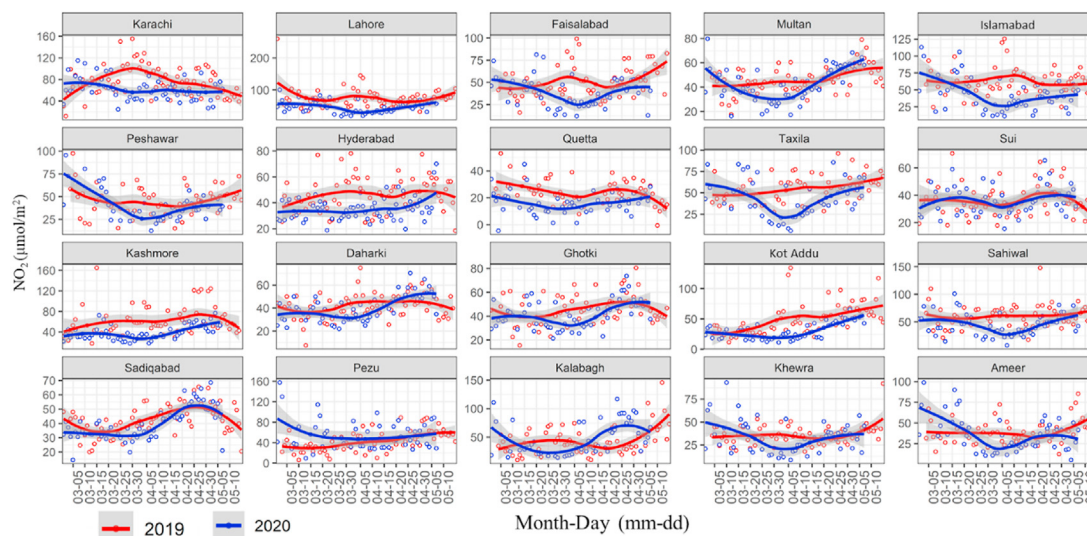
Fig. 4. Time series plots of the tropospheric NO_2 concentration from March 01 to May 15 in 2019 and 2020 epochs across various stages of lockdown. The red and blue circles indicate the NO_2 values in 2019 and 2020, lines indicate loess fitted curves and the shaded grey colour show 95% confidence interval. (For interpretation of the references to colour in this figure legend, the reader is referred to the Web version of this article.)
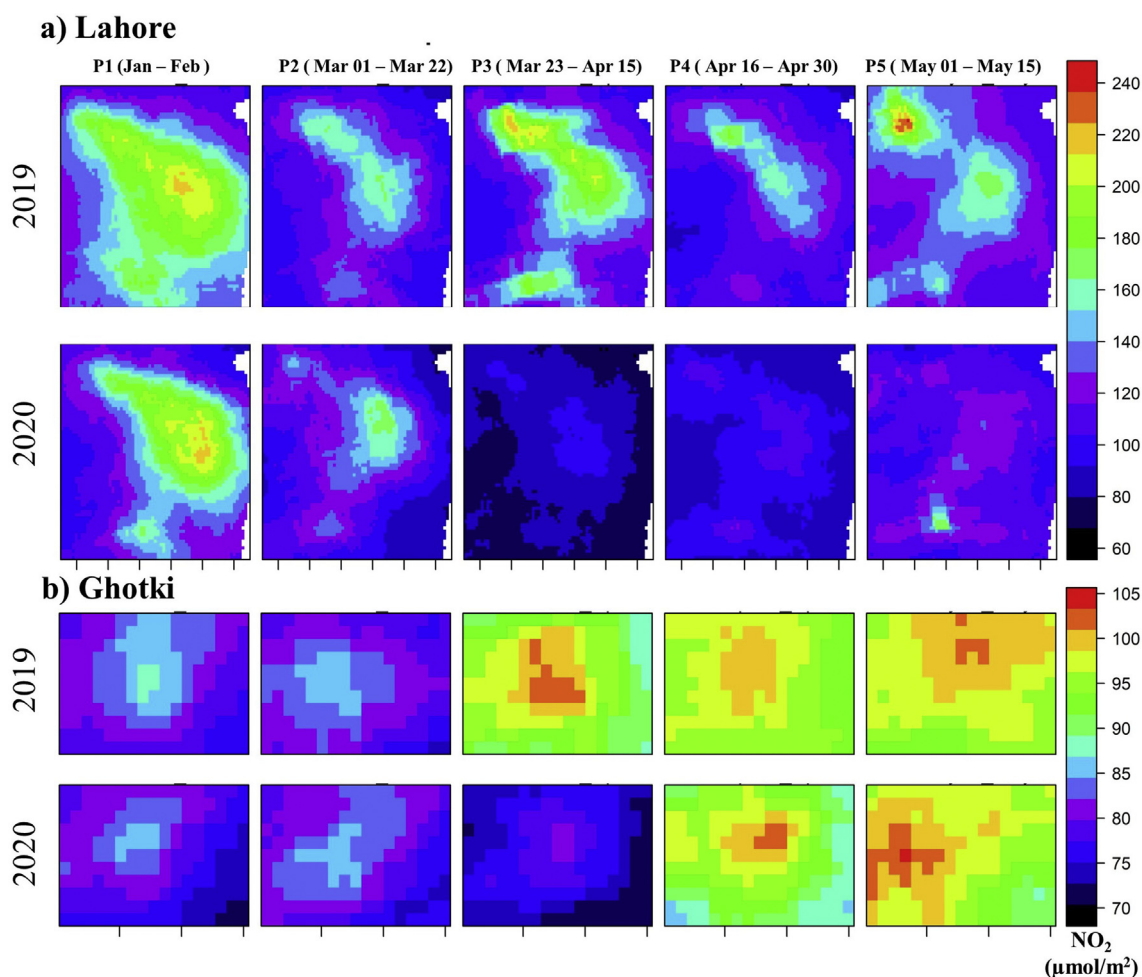

Fig. 5. Typified insets of different NO_2 recovery trajectories in a megacity (a-Lahore) and a gas field plant (b - in Ghotki).

during the pandemic without pause. The gas fields in Daharki and Ghotki were closed but for a shorter period (P3- March 23 to April 15)

compared to other industrial activities Fig. 4.

3.3. Lockdown impact on CO and SO₂

Apart from the drastic decrease in NO_2, the comparison of atmospheric CO concentration during the lockdown in 2020 with similar period in 2019 showed a significant decrease ($p < 0.05$) over all the megacities, except Karachi (Fig. 6). Similarly, the industrial region of Taxila and gas field in Ghotki indicated a significant drop in CO values during the lockdown period. Notably, a very significant ($p = 0.0049$) drop in CO concentration was observed over the Sahiwal coal power plant. All the cement plants in Pezu, Kalabagh, Khewra, and Ameer showed a reduction in the concentration of CO during the lockdown period indicating that these cement plants are main contributors of the CO emission in the country. Influence of Sahiwal power plant to both NO_2 and CO is noteworthy which require further investigation. Yuan et al. (2021), observed a 30% decline of CO concentration in the megacity of Hangzhou in the Yangtze River Delta in eastern China. A nation-wide decline in CO due to COVID-19 lockdown is also reported in Republic of Korea (Ju et al., 2021) where higher concentrations of CO in urban and urban industrial areas are observed as compared to sub-urban regions.

We did not observe significant changes in SO_2 due to the lockdown in Pakistan (please see appendix Fig A1) that is in line with another study conducted in Republic of Korea (Ju et al., 2021) but contradicts to the observed 83% decline in SO_2 in Hangzhou (eastern China) during the lockdown (Yuan et al., 2021).

3.4. Lockdown impact on AOD

Observations during the period of Jan—May 2019 suggest that AOD is highest over the gas field plants at Ghotki ($0.515 \ \mu g/cm^2$) in

northern Sindh followed by Sui ($0.513 \ \mu g/cm^2$) in northern Baluchistan, the Kashmore power plant ($0.41 \ \mu g/cm^2$), and the industrial areas of Sadiqabad ($0.433 \ \mu g/cm^2$) (Table 1, Fig. 7). Interestingly, among the mega and major cities, the average AOD is highest in Multan ($0.357 \ \mu g/cm^2$) which is a not a megacity, followed by another major city Hyderabad ($0.353 \ \mu g/cm^2$). Among the megacities, AOD is highest in Faisalabad ($0.345 \ \mu g/cm^2$), which is also one of the mega industrial cities of Pakistan, followed by Lahore ($0.342 \ \mu g/cm^2$) and Karachi ($0.338 \ \mu g/cm^2$) (Table 1, Fig. 7). Previous studies have suggested an increase in AOD from winter to summer (Alam et al., 2010; Gupta et al., 2013) although this temporal increase becomes visible only from the last quarter of April. Mansha (2011), who characterized air $PM_{2.5}$ in the industrial city of Karachi, has shown that industrial emissions contribute more than 50% of it followed by dust and secondary aerosols. Studies undertaken in Lahore have suggested that fossil fuel and biomass burning are the major sources of carbonaceous aerosols (Khanum et al., 2017; Mansha, 2011).

The reduction in industrial and human activities during the lockdown has led to a drop in aerosol levels in most of the places albeit for a short interval and with varying intensities. Among the 20 locations, an increase in AOD is observed at 5 sites although both the increase and decrease are not statistically significant (Fig. 8). Such variability can be linked to remote sensing-based AOD measurement sensitivity to weather patterns (Kourtidis et al., 2015). Since aerosol particle concentration correlates better with CO than with SO_2 and NO_2, we analyzed Sentinel 5P CO concentration for the lockdown period and observed consistently low emissions during 2020 (Fig. 6). Moreover, the aggregated AOD concentration decreased, compared to 2019, during the lockdown periods, P-3
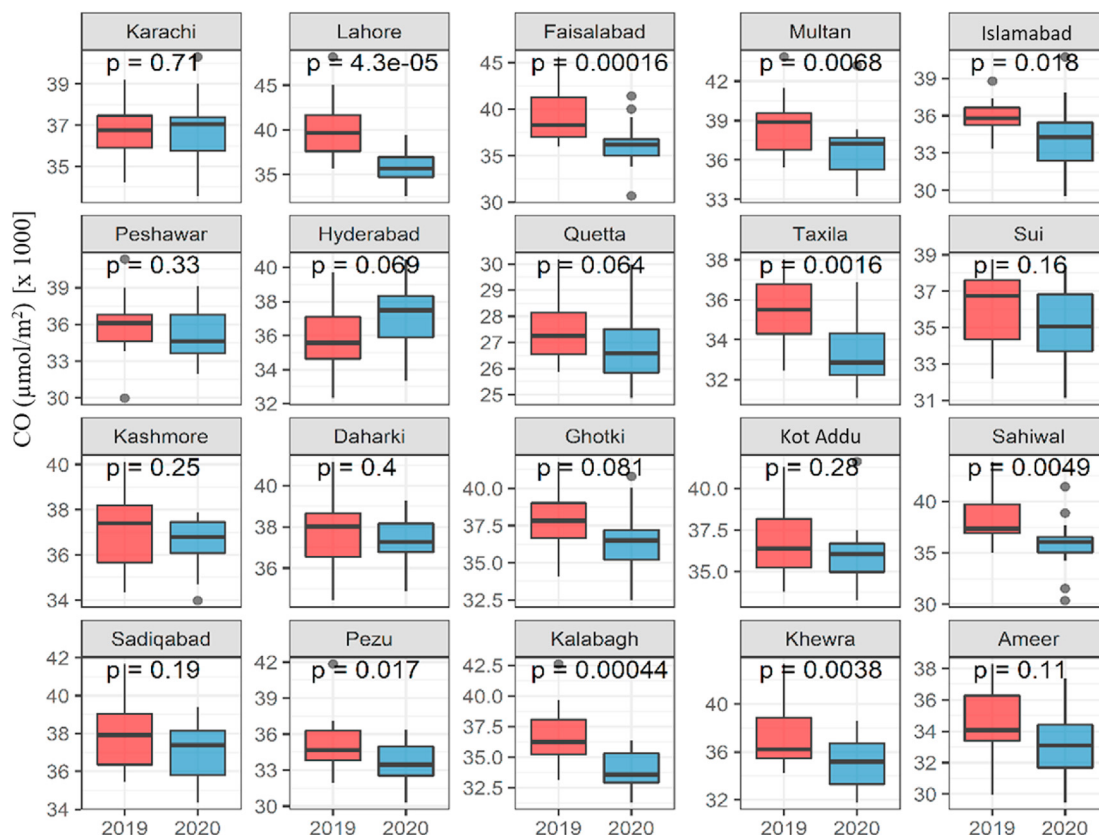

Fig. 6. Change in CO concentration during March 23 − April 15 in 2019 and 2020. The red and blue colours refer to the year 2019 and 2020, respectively. (For interpretation of the references to colour in this figure legend, the reader is referred to the Web version of this article.)
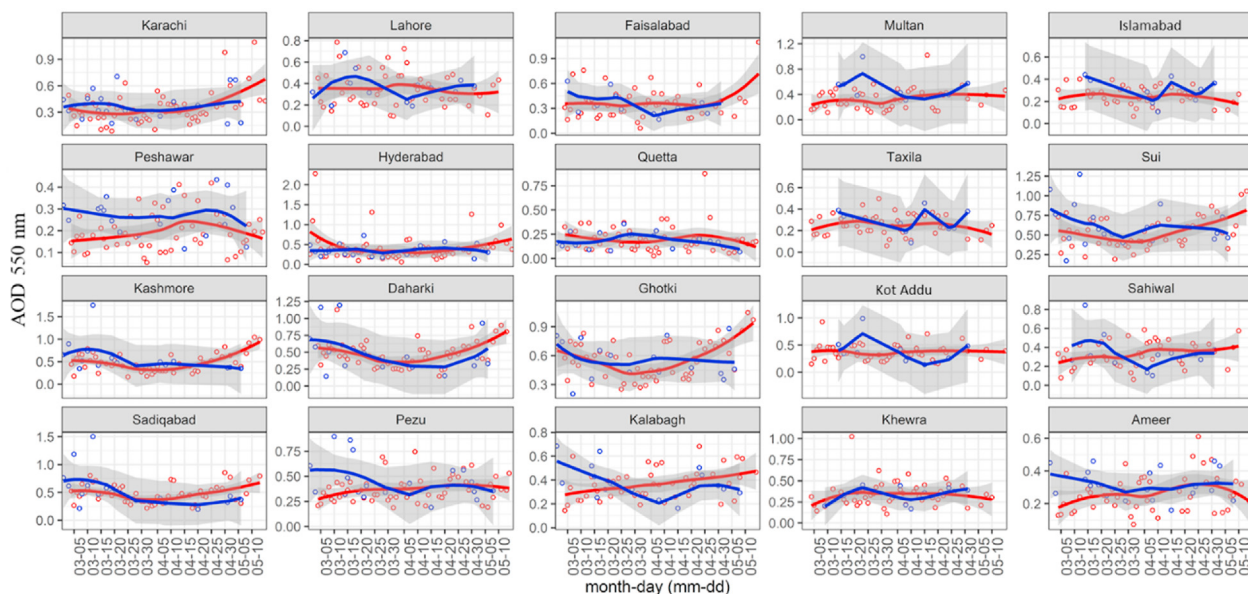
Fig. 7. Changes in the AOD thickness across various stages of lockdown. The red and blue circles indicate the AOD values in 2019 and 2020, lines indicate loess fitted curves, and the shaded grey colour shows a 95% confidence interval. (For interpretation of the references to colour in this figure legend, the reader is referred to the Web version of this article.)
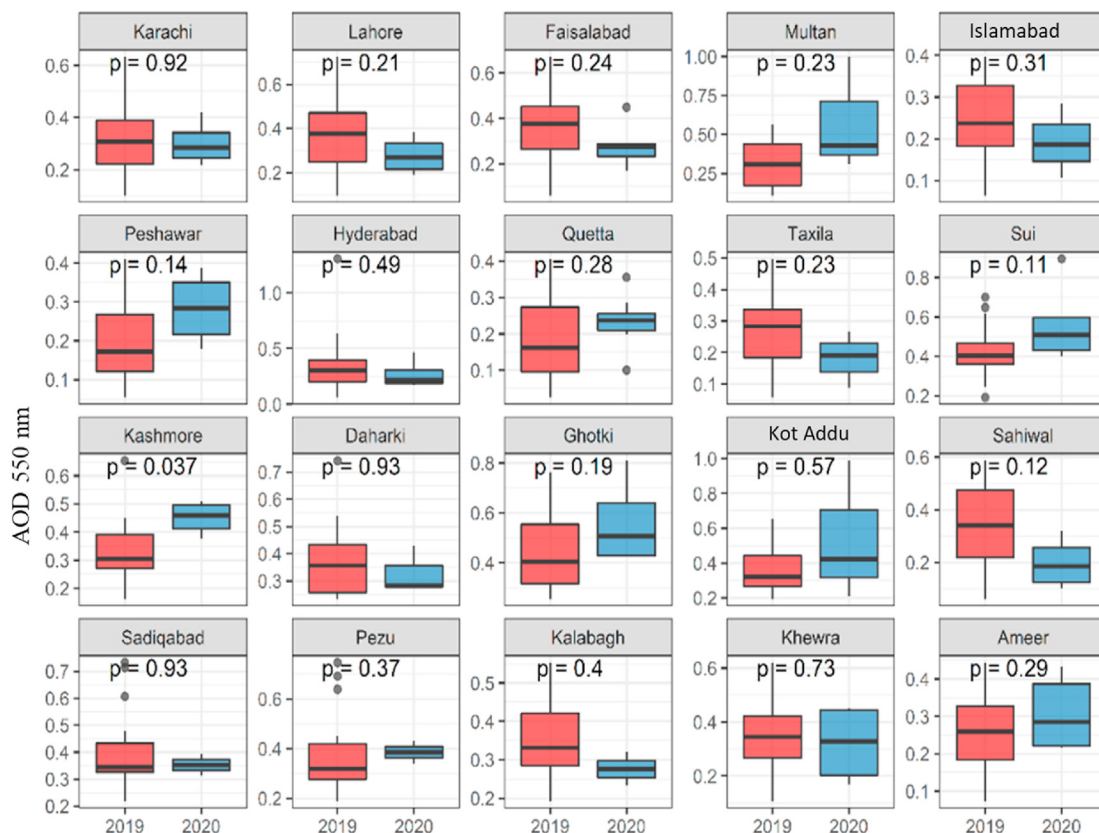

Fig. 8. Change in AOD thickness during March 23 − April 15 in 2019 and 2020. Red and blue colours refer to the year 2019 and 2020, respectively. (For interpretation of the references to colour in this figure legend, the reader is referred to the Web version of this article.)

(March 22 to April 15) and P- 4 (April 16 to April 30). We observed an especially significant reduction over gas fields (29% decrease) and industrial (25% decrease) and power plant (23% decrease) regions (Fig. 8, Table 1).

3.5. Lockdown impact on SUHI effect

Fig. 9 shows the average SUHI effect of the eight mega-city centres of Pakistan during the five periods in 2019 and 2020. The SUHI analysis is confined to large cities with at least 1 million
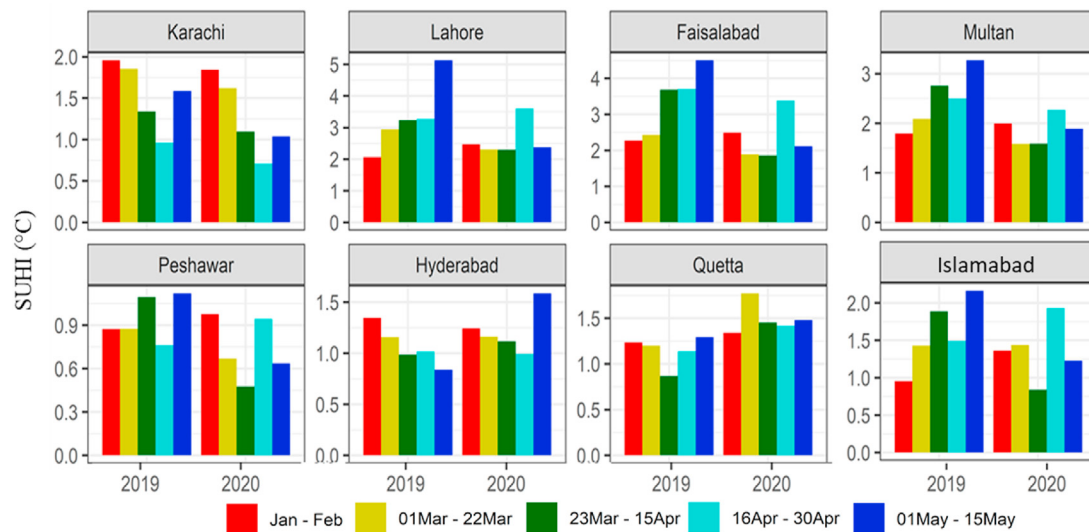
Fig. 9. Average SUHI conditions from January to May during 2019 and 2020 across major cities of Pakistan.

population with a significant proportion of impervious surfaces/built-up areas. It shows that, during P3 and P4 from March 23 to April 30, the average drop in the SUHI of megacities was 20% (from 2.4 °C in 2019 to 2.0 °C in 2020) while it is 18% and 11% in the major cities i.e., Multan (from 2.6 °C in 2019 to 1.9 °C in 2020) and Peshawar (from 0.9 °C in 2019 to 0.7 °C in 2020) (Table 1, Fig. 9). Among the megacities, the most significant drop in SUHI is observed in Faisalabad (29% decrease from 3.7 °C in 2019 to 2.6 °C in 2020) followed by Karachi (22% decrease from 1.2 °C in 2019 to 0.9 °C in 2020) and Islamabad-Rawalpindi (18% decrease from 1.7 °C in 2019 to 0.4 °C in 2020). The general temporal patterns show an overall reduction in SUHI in 2020 for all the periods. The drop in the SUHI or LST in the cities is notable, though not very significant, during 2020 which could be attributed to both the lockdown and the generally cooler weather pattern. Such a drop in SUHI could be a useful indicator for policymakers in attempts to control the increasing temperature in cities. Rizvi et al. (2019) have observed a 1.9 °C increase in temperature in the SUHI effect in Karachi during the last 18 years with an increasing trend in recent years. Shah and Ghauri (2015) have attributed the increasing SUHI trends to urban expansion during the period between 2000 and 2011 in Lahore. But a substantial reduction in SUHI conditions in the major cities of Pakistan was observed during the lockdown period (Fig. 9) because the road traffic slowed to a trickle after everyone in the country except essential workers was required to stay at home. Overall, the reduction in megacities was higher than in other large cities (Table 1, Fig. 9). This reduction during the complete and partial lockdown periods signifies the added contribution of the transportation sector along with the widely known land-use influences to SUHI effect (Kardinal Jusuf et al., 2007; Singh et al., 2017).

4. Conclusions

This study used the satellite remote sensing-based assessment of pollution emissions to evaluate changes in nitrogen dioxide (NO_2), carbon monoxide (CO), sulphur dioxide (SO_2), aerosol optical depth (AOD) and the surface urban heat island (SUHI) effect induced by the lockdown countrywide to minimize the spread of the COVID-19 virus in Pakistan. The results indicate that the halt in energy consumption by human and industrial activities significantly reduced emissions though to varying degrees across

different sectors and sources of emission. The highest amount of reduction in NO_2 emissions was recorded over coal-based thermal power plants followed by megacities where emissions were a combination of transportation and industrial sources. The changes in AOD, in contrast, were highly erratic across the study sites and statistically less significant. Overall, AOD thickness reduction was highest over gas fields followed by thermal power plants. In the case of urban areas, while an increase in AOD thickness is observed in the major cities, only a small reduction is observed in the megacities. The reported changes, as well as the methods applied in our study, provide a basis to assess the sectoral pollution contributions to air quality in the absence of ground-based monitoring systems. Additionally, this study assesses the impact of the halt in transportation on the SUHI phenomenon in the major urban centres of Pakistan. The findings indicate a notable decrease in the SUHI effect in megacities during the lockdown although changes in major cities were negligible. The unforeseen and unprecedented disruption to anthropic activities due to the pandemic-induced lockdown gave the researchers an invaluable opportunity to identify the sectoral contributions to air pollution emissions in Pakistan. The findings highlight the need for appropriate management of transportation systems, land use expansion, use of renewable energy, and industrial emissions to tackle the urban surface energy balance. Future research could evaluate the environmental cost of energy production and its use across various sectors in Pakistan and to develop appropriate environmental policies to reduce emissions.

CRediT authorship contribution statement

Ghaffar Ali: Writing - review & editing, Visualization. **Sawaid Abbas:** Conceptualization, Formal analysis, Writing - review & editing. **Faisal Mueen Qamer:** Conceptualization, Writing - original draft. **Man Sing Wong:** Supervision. **Ghulam Rasul:** Quality and Validation. **Syed Muhammad Irteza:** Validation. **Naeem Shahzad:** Writing - review & editing.

Declaration of competing interest

The authors declare that they have no known competing financial interests or personal relationships that could have appeared to influence the work reported in this paper.

Acknowledgements

Appendix A. Supplementary data

Supplementary data to this article can be found online at https://doi.org/10.1016/j.jclepro.2021.125806.

References

Alam, K., Iqbal, M.J., Blaschke, T., Qureshi, S., Khan, G., 2010. Monitoring spatio-temporal variations in aerosols and aerosol−cloud interactions over Pakistan using MODIS data. Adv. Space Res. 46, 1162−1176. https://doi.org/10.1016/j.asr.2010.06.025.

Alkon, M., He, X., Paris, A.R., Liao, W., Hodson, T., Wanders, N., Wang, Y., 2019. Water security implications of coal-fired power plants financed through China's Belt and Road Initiative. Energy Pol. 132, 1101−1109. https://doi.org/10.1016/j.enpol.2019.06.044.

Asian Development Bank, 2020. The economic impact of the COVID-19 outbreak on developing Asia. Asian Dev. Bank 9, 1−14. https://doi.org/10.22617/BRF200096.

Bilal, M., Nichol, J.E., Spak, S.N., 2017. A new approach for estimation of fine particulate concentrations using satellite aerosol optical depth and binning of meteorological variables. Aerosol Air Qual. Res. 17, 356−367. https://doi.org/10.4209/aaqr.2016.03.0097.

Buchhorn, M., Smets, B., Bertels, L., Lesiv, M., Tsendbazar, N.-E., Herold, M., Fritz, S., 2019. Copernicus Global Land Service: Land Cover 100m: Epoch 2015. Globe. https://doi.org/10.5281/zenodo.3243509.

Butt, F.M., Shahzad, M.I., Khalid, S., Iqbal, N., Rasheed, A., Raza, G., 2018. Comparison of aerosol optical depth products from multi-satellites over densely populated cities of Pakistan. Int. Lett. Nat. Sci. 69, 12−24. https://doi.org/10.18052/www.scipress.com/ILNS.69.12.

Chapman, L., Thornes, J.E., 2005. The influence of traffic on road surface temperatures: implications for thermal mapping studies. Meteorol. Appl. 12, 371. https://doi.org/10.1017/S1350482705001957.

Colbeck, I., Nasir, Z.A., Ali, Z., 2010. The state of ambient air quality in Pakistan—a review. Environ. Sci. Pollut. Res. 17, 49−63. https://doi.org/10.1007/s11356-009-0217-2.

Corbane, C., Pesaresi, M., Politis, P., Syrris, V., Florczyk, A.J., Soille, P., Maffenini, L., Burger, A., Vasilev, V., Rodriguez, D., Sabo, F., Dijkstra, L., Kemper, T., 2017. Big earth data analytics on Sentinel-1 and Landsat imagery in support to global human settlements mapping. Big Earth Data 1, 118−144. https://doi.org/10.1080/20964471.2017.1397899.

Fatmi, Z., Ntani, G., Coggon, D., 2020. Levels and determinants of fine particulate matter and carbon monoxide in kitchens using biomass and non-biomass fuel for cooking. Int. J. Environ. Res. Publ. Health 17, 1287. https://doi.org/10.3390/ijerph17041287.

Gorelick, N., Hancher, M., Dixon, M., Ilyushchenko, S., Thau, D., Moore, R., 2017. Google earth engine: planetary-scale geospatial analysis for everyone. Remote Sens. Environ. 202, 18−27. https://doi.org/10.1016/j.rse.2017.06.031.

Griffin, D., Zhao, X., McLinden, C.A., Boersma, F., Bourassa, A., Dammers, E., Degenstein, D., Eskes, H., Fehr, L., Fioletov, V., Hayden, K., Kharol, S.K., Li, S.-M., Makar, P., Martin, R.V., Mihele, C., Mittermeier, R.L., Krotkov, N., Sneep, M., Lamsal, L.N., Linden, M. ter, Geffen, J. van, Veefkind, P., Wolde, M., 2019. High-resolution mapping of nitrogen dioxide with TROPOMI: first results and validation over the Canadian oil sands. Geophys. Res. Lett. 46, 1049−1060. https://doi.org/10.1029/2018GL081095.

Gupta, P., Khan, M.N., da Silva, A., Patadia, F., 2013. MODIS aerosol optical depth observations over urban areas in Pakistan: quantity and quality of the data for air quality monitoring. Atmos. Pollut. Res. 4, 43−52. https://doi.org/10.5094/APR.2013.005.

Hussain, M., Akhtar, F., Khan, S.S., 2018. Impact and ratio of lead in ambient air from vehicular emission in Quetta valley, Pakistan. IOP Conf. Ser. Mater. Sci. Eng. 414, 012044 https://doi.org/10.1088/1757-899X/414/1/012044.

Ialongo, I., Virta, H., Eskes, H., Hovila, J., Douros, J., 2020. Comparison of TROPOMI/Sentinel-5 Precursor NO$_2$ observations with ground-based measurements in Helsinki. Atmos. Meas. Tech. 13, 205−218. https://doi.org/10.5194/amt-13-205-2020.

IQAir, 2019. World Air Quality. 2019 World Air Qual. Rep, pp. 1−22.

Isaifan, R.J., 2020. The dramatic impact of Coronavirus outbreak on air quality: has it saved as much as it has killed so far? Glob. J. Environ. Sci. Manag. 6, 275−288. https://doi.org/10.22034/GJESM.2020.03.01.

Jabeen, Z., Khokhar, M.F., 2019. Extended database of SO2 column densities over Pakistan by exploiting satellite observations. Atmos. Pollut. Res. 10, 997−1003. https://doi.org/10.1016/j.apr.2019.01.009.

Ju, M.J., Oh, J., Choi, Y.H., 2021. Changes in air pollution levels after COVID-19 outbreak in Korea. Sci. Total Environ. 750, 141521. https://doi.org/10.1016/j.scitotenv.2020.141521.

Kaplan, G., Avdan, Z.Y., Avdan, U., 2019. Spaceborne nitrogen dioxide observations from the sentinel-5P TROPOMI over Turkey. In: Wang, Q. (Ed.), 3rd International Electronic Conference on Remote Sensing. MDPI, Proceedings, Online, p. 4. https://doi.org/10.3390/ECRS-3-06181.

Kardinal Jusuf, S., Wong, N.H., Hagen, E., Anggoro, R., Hong, Y., 2007. The influence of land use on the urban heat island in Singapore. Habitat Int. 31, 232−242. https://doi.org/10.1016/j.habitatint.2007.02.006.

Khanum, F., Chaudhry, M.N., Kumar, P., 2017. Characterization of five-year observation data of fine particulate matter in the metropolitan area of Lahore. Air Qual. Atmos. Heal. 10, 725−736. https://doi.org/10.1007/s11869-017-0464-1.

Kim, J., Jeong, U., Ahn, M., Kim, J.H., Park, R.J., Lee, Hanlim, Song, C.H., Choi, Y.-S., Lee, K.-H., Yoo, J., Jeong, M., Park, S.K., Lee, K.-M., Song, C., Kim, Sang-Woo, Kim, Y.J., Kim, Si-Wan, Kim, M., Go, S., Liu, X., Chance, K., Chan Miller, C., Al-Saadi, J., Veihelmann, B., Bhartia, P.K., Torres, O., Abad, G.G., Haffner, D.P., Ko, D.H., Lee, S.H., Woo, J., Chong, H., Park, S.S., Nicks, D., Choi, W.J., Moon, K., Cho, A., Yoon, J., Kim, S., Hong, H., Lee, K., Lee, Hana, Lee, S., Choi, M., Veefkind, P., Levelt, P.F., Edwards, D.P., Kang, M., Eo, M., Bak, J., Baek, K., Kwon, H.-A., Yang, J., Park, J., Han, K.M., Kim, B., Shin, H., Choi, H., Lee, E., Chong, J., Cha, Y., Koo, J., Irie, H., Hayashida, S., Kasai, Y., Kanaya, Y., Liu, C., Lin, J., Crawford, J.H., Carmichael, G.R., Newchurch, M.J., Lefer, B.L., Herman, J.R., Swap, R.J., Lau, A.K.H., Kurosu, T.P., Jaross, G., Ahlers, B., Dobber, M., McElroy, C.T., Choi, Y., 2020. new era of air quality monitoring from space: geostationary environment monitoring spectrometer (GEMS). Bull. Am. Meteorol. Soc. 101, E1−E22. https://doi.org/10.1175/BAMS-D-18-0013.1.

Kourtidis, K., Stathopoulos, S., Georgoulias, A.K., Alexandri, G., Rapsomanikis, S., 2015. A study of the impact of synoptic weather conditions and water vapor on aerosol−cloud relationships over major urban clusters of China. Atmos. Chem. Phys. 15, 10955−10964. https://doi.org/10.5194/acp-15-10955-2015.

Krishna, R.K., Ghude, S.D., Kumar, R., Beig, G., Kulkarni, R., Nivdange, S., Chate, D., 2019. Surface PM2.5 estimate using satellite-derived aerosol optical depth over India. Aerosol Air Qual. Res. 19, 25−37. https://doi.org/10.4209/aaqr.2017.12.0568.

Lama, S., Houweling, S., Boersma, K.F., Aben, I., van der Gon, H.A.C.D., Krol, M.C., Dolman, H., Borsdorff, T., Lorente, A., 2019. Quantifying burning efficiency in megacities using NO2/CO ratio from the tropospheric monitoring instrument (TROPOMI). Atmos. Chem. Phys. Discuss. 1, 1−22. https://doi.org/10.5194/acp-2019-1112.

Le Quéré, C., Jackson, R.B., Jones, M.W., Smith, A.J.P., Abernethy, S., Andrew, R.M., De-Gol, A.J., Willis, D.R., Shan, Y., Canadell, J.G., Friedlingstein, P., Creutzig, F., Peters, G.P., 2020. Temporary reduction in daily global CO2 emissions during the COVID-19 forced confinement. Nat. Clim. Change. https://doi.org/10.1038/s41558-020-0797-x.

Levy, R.C., Remer, L.A., Kleidman, R.G., Mattoo, S., Ichoku, C., Kahn, R., Eck, T.F., 2010. Global evaluation of the Collection 5 MODIS dark-target aerosol products over land. Atmos. Chem. Phys. 10, 10399−10420. https://doi.org/10.5194/acp-10-10399-2010.

Lyapustin, A., Wang, Y., 2018. MCD19A2 MODIS/Terra+Aqua Land Aerosol Optical Depth Daily L2G Global 1km SIN Grid V006 [Data set] [WWW Document]. NASA EOSDIS L. Process. DAAC. https://doi.org/10.5067/MODIS/MCD19A2.006.

Maliszewska, M., Mattoo, A., Mensbrgghe, D., 2020. The Potential Impact of COVID-19 on GDP and Trade A Preliminary Assessment (English), Policy Research Working Paper; No. WPS 9211; COVID-19 (Coronavirus). Washington, D.C.

Mansha, M., 2011. Assessment of fine particulate matter (PM$_{2.5}$) in metropolitan Karachi through satellite and ground−based measurements. J. Appl. Remote Sens. 5, 053546 https://doi.org/10.1117/1.3625615.

Mao, K.B., Ma, Y., Xia, L., Chen, W.Y., Shen, X.Y., He, T.J., Xu, T.R., 2014. Global aerosol change in the last decade: an analysis based on MODIS data. Atmos. Environ. 94, 680−686. https://doi.org/10.1016/j.atmosenv.2014.04.053.

Martin-Vide, J., Sarricolea, P., Moreno-Garcᾱa, M.C., 2015. On the definition of urban heat island intensity: the â€œruralâ€ reference. Front. Earth Sci. 3 https://doi.org/10.3389/feart.2015.00024.

NEPRA, 2020. State of Industry Report 2020.

Neteler, M., 2010. Estimating daily land surface temperatures in mountainous environments by reconstructed MODIS LST data. Rem. Sens. 2, 333−351. https://doi.org/10.3390/rs1020333.

Nori-Sarma, A., Benmarhnia, T., Rajiva, A., Azhar, G.S., Gupta, P., Pednekar, M.S., Bell, M.L., 2019. Advancing our understanding of heat wave criteria and associated health impacts to improve heat wave alerts in developing country settings. Int. J. Environ. Res. Publ. Health 16, 2089. https://doi.org/10.3390/ijerph16122089.

Omrani, H., Omrani, B., Parmentier, B., Helbich, M., 2020. Spatio-temporal data on the air pollutant nitrogen dioxide derived from Sentinel satellite for France. Data Br 28, 105089. https://doi.org/10.1016/j.dib.2019.105089.

Phelan, P.E., Kaloush, K., Miner, M., Golden, J., Phelan, B., Silva, H., Taylor, R.A., 2015. Urban heat island: mechanisms, implications, and possible remedies. Annu. Rev. Environ. Resour. 40, 285–307. https://doi.org/10.1146/annurev-environ-102014-021155.

Pilarczyk, M., Węglowski, B., Nord, L.O., 2019. A comprehensive thermal and structural transient analysis of a boiler's steam outlet header by means of a dedicated algorithm and FEM simulation. Energies 13, 111. https://doi.org/10.3390/en13010111.

R Core Team, 2020. R: A Language and Environment for Statistical Computing. R Foundation for Statistical Computing, Vienna, Austria.

S5P-Gee, 2020. COPERNICUS S5P Description [WWW Document]. https://developers.google.com/earth-engine/datasets/catalog/COPERNICUS_S5P_OFFL_L3_NO2#description.

Saadat, S., Rawtani, D., Hussain, C.M., 2020. Environmental perspective of COVID-19. Sci. Total Environ. 728, 138870. https://doi.org/10.1016/j.scitotenv.2020.138870.

Sánchez-Triana, E., Enriquez, S., Afzal, J., Nakagawa, A., Khan, A.S., 2014. Cleaning Pakistan's Air: Policy Options to Address the Cost of Outdoor Air Pollution. The World Bank. https://doi.org/10.1596/978-1-4648-0235-5.

Shah, B., Ghauri, B., 2015. Mapping urban heat island effect in comparison with the land use, land cover of lahore district. Pakistan J. Meteorol. 11, 37–48.

Shahid, M.Z., Hong, L., Yu-lu, Q.I.U., Shahid, I., 2015. Source sector contributions to aerosol levels in Pakistan. Atmos. Oceanogr. Sci. Libr. 8, 308–313. https://doi.org/10.3878/AOSL20150049.

Shikwambana, L., Mhangara, P., Mbatha, N., 2020. Trend analysis and first time observations of sulphur dioxide and nitrogen dioxide in South Africa using TROPOMI/Sentinel-5 P data. Int. J. Appl. Earth Obs. Geoinf. 91, 102130. https://doi.org/10.1016/j.jag.2020.102130.

Singh, P., Kikon, N., Verma, P., 2017. Impact of land use change and urbanization on urban heat island in Lucknow city, Central India. A remote sensing based estimate. Sustain. Cities Soc. 32, 100–114. https://doi.org/10.1016/j.scs.2017.02.018.

TROPMI, 2020. TROPMI: Data Products [WWW Document]. http://www.tropomi.eu/data-products/level-2-products.

Veefkind, J.P., Aben, I., McMullan, K., Förster, H., de Vries, J., Otter, G., Claas, J., Eskes, H.J., de Haan, J.F., Kleipool, Q., van Weele, M., Hasekamp, O., Hoogeveen, R., Landgraf, J., Snel, R., Tol, P., Ingmann, P., Voors, R., Kruizinga, B., Vink, R., Visser, H., Levelt, P.F., 2012. TROPOMI on the ESA Sentinel-5 Precursor: a GMES mission for global observations of the atmospheric composition for climate, air quality and ozone layer applications. Remote Sens. Environ. 120, 70–83. https://doi.org/10.1016/j.rse.2011.09.027.

Yuan, Q., Qi, B., Hu, D., Wang, J., Zhang, J., Yang, H., Zhang, S., Liu, L., Xu, L., Li, W., 2021. Spatiotemporal variations and reduction of air pollutants during the COVID-19 pandemic in a megacity of Yangtze River Delta in China. Sci. Total Environ. 751, 141820. https://doi.org/10.1016/j.scitotenv.2020.141820.

Yunus, A.P., Masago, Y., Hijioka, Y., 2020. COVID-19 and surface water quality: improved lake water quality during the lockdown. Sci. Total Environ. 731, 139012. https://doi.org/10.1016/j.scitotenv.2020.139012.

Zhang, R., Zhang, Y., Lin, H., Feng, X., Fu, T., Wang, Y., 2020. NOx emission reduction and recovery during COVID-19 in east China. Atmosphere (Basel) 11, 433. https://doi.org/10.3390/atmos11040433.

Zheng, Yang, Wu, Marinello, 2019. Spatial variation of NO2 and its impact factors in China: an application of sentinel-5P products. Rem. Sens. 11, 1939. https://doi.org/10.3390/rs11161939.

Zhu, R., Wong, M.S., Guilbert, É., Chan, P., 2017. Understanding heat patterns produced by vehicular flows in urban areas. Sci. Rep. 7, 16309. https://doi.org/10.1038/s41598-017-15869-6.